



HAL
open science

Energy Cascade Rate Measured in a Collisionless Space Plasma with MMS Data and Compressible Hall Magnetohydrodynamic Turbulence Theory

Nahuel Andrés, Fouad Sahraoui, Sébastien Galtier, Lina Hadid, R. Ferrand,
S.Y. Huang

► **To cite this version:**

Nahuel Andrés, Fouad Sahraoui, Sébastien Galtier, Lina Hadid, R. Ferrand, et al.. Energy Cascade Rate Measured in a Collisionless Space Plasma with MMS Data and Compressible Hall Magnetohydrodynamic Turbulence Theory. *Physical Review Letters*, 2019, 123 (24), pp.055102. 10.1103/PhysRevLett.123.245101 . hal-02724598

HAL Id: hal-02724598

<https://hal.science/hal-02724598>

Submitted on 16 Sep 2022

HAL is a multi-disciplinary open access archive for the deposit and dissemination of scientific research documents, whether they are published or not. The documents may come from teaching and research institutions in France or abroad, or from public or private research centers.

L'archive ouverte pluridisciplinaire **HAL**, est destinée au dépôt et à la diffusion de documents scientifiques de niveau recherche, publiés ou non, émanant des établissements d'enseignement et de recherche français ou étrangers, des laboratoires publics ou privés.

Energy Cascade Rate Measured in a Collisionless Space Plasma with MMS Data and Compressible Hall Magnetohydrodynamic Turbulence Theory

N. Andrés^{1,2,3,*}, F. Sahraoui,¹ S. Galtier^{1,4}, L. Z. Hadid,⁵ R. Ferrand,¹ and S. Y. Huang⁶

¹Laboratoire de Physique des Plasmas, École Polytechnique, CNRS, Sorbonne University,

Observatoire de Paris, Univ. Paris-Sud, F-91128 Palaiseau Cedex, France

²Instituto de Astronomía y Física del Espacio, CONICET-UBA, Ciudad Universitaria, 1428, Buenos Aires, Argentina

³Departamento de Física, Facultad de Ciencias Exactas y Naturales, UBA, Ciudad Universitaria, 1428, Buenos Aires, Argentina

⁴Institut Universitaire de France (IUF), 2201 France

⁵European Space Agency, ESTEC, 75231 Noordwijk, Netherlands

⁶School of Electronic and Information, Wuhan University, 430072 Wuhan, China



(Received 9 August 2019; revised manuscript received 12 November 2019; published 13 December 2019)

The first complete estimation of the compressible energy cascade rate $|\varepsilon_C|$ at magnetohydrodynamic (MHD) and subion scales is obtained in Earth's magnetosheath using Magnetospheric MultiScale spacecraft data and an exact law derived recently for *compressible* Hall MHD turbulence. A multispacecraft technique is used to compute the velocity and magnetic gradients, and then all the correlation functions involved in the exact relation. It is shown that when the density fluctuations are relatively small, $|\varepsilon_C|$ identifies well with its incompressible analog $|\varepsilon_I|$ at MHD scales but becomes much larger than $|\varepsilon_I|$ at subion scales. For larger density fluctuations, $|\varepsilon_C|$ is larger than $|\varepsilon_I|$ at every scale with a value significantly higher than for smaller density fluctuations. Our study reveals also that for both small and large density fluctuations, the nonflux terms remain always negligible with respect to the flux terms and that the major contribution to $|\varepsilon_C|$ at subion scales comes from the compressible Hall flux.

DOI: 10.1103/PhysRevLett.123.245101

Introduction.—Turbulence is a universal phenomenon observed from quantum to astrophysical scales, see, e.g., Refs. [1–3]. It is mainly characterized by a nonlinear transfer (or cascade) of energy from a source to a sink. In astrophysical plasmas, fully developed turbulence plays a major role in several physical processes such as accretion flows around massive objects, star formation, solar wind heating, or energy transport in planetary magnetospheres [4–7]. In particular, Earth's magnetosheath (MS)—the region of the solar wind downstream of the bow shock [8]—provides a unique laboratory to investigate *compressible* plasma turbulence. Indeed, a key feature of the MS plasma is the high level of density fluctuations in it, which can reach up to 100% of the background density [9–11], in contrast to the solar wind, where it is $\sim 20\%$ [12,13]. Thanks to the high time resolution data provided by the Magnetospheric MultiScale (MMS) mission in Earth's MS [14], we are now able for the first time to measure the compressible energy cascade rate ε_C from the magnetohydrodynamic (MHD) inertial range down to the subion scales.

The energy cascade rates can be estimated using exact laws derived from fluid models which relate, in the simplest case, the longitudinal structure functions of the turbulent variables (e.g., the velocity field \mathbf{u} or the magnetic field \mathbf{B}) taken in two points, to the spatial increment ℓ that separates them. The first exact relation

for a plasma was derived by Politano and Pouquet [15,16] (hereafter PP98): it describes three-dimensional (3D) incompressible MHD (IMHD) turbulence under the assumption of statistical homogeneity and isotropy. This law has been the subject of several numerical tests, see, e.g., Refs. [17–19]; it has been used for the evaluation of the incompressible cascade rates in space plasmas [20–22] (denoted here $\varepsilon_{\text{IMHD}}$) and the magnetic or kinetic Reynolds numbers [23], and for the large-scale modeling of the solar wind [24,25].

The IMHD approximation has been successfully used to study plasma turbulence at scales larger than the ion inertial length d_i (or the Larmor radius ρ_i) [4,26]. However, at spatial scales comparable or smaller than d_i , the ions are no longer frozen-in to the magnetic field lines because of the Hall term in the generalized Ohm's law, e.g., Ref. [8]. Moreover, the incompressibility assumption is likely to fail to describe subion scales physics: it is theoretically justified at MHD scales because of the existence of a purely incompressible Alfvén wave solution. However, that mode becomes a kinetic Alfvénic wave (KAW) at subion scales, which is inherently compressible since it carries density fluctuations [5,27]. A nearly incompressible whistler mode can develop at high frequency [28], but that mode is unlikely to dominate the subion scales cascade in the solar wind or MS [5,29–31]. These considerations emphasize the crucial need to incorporate density fluctuations in the

description of the subion scale cascade, as we will show below using MMS data in the MS.

Following the same methodology as in Ref. [32], Banerjee and Galtier [33] derived an exact law for isothermal compressible MHD (CMHD) turbulence. Recently, Andrés and Sahraoui [34] revisited that work by providing an alternative derivation of the exact law that relates the compressible energy cascade rate (hereafter $\varepsilon_{\text{CMHD}}$) to four different categories of terms, namely, the source, hybrid, and β dependent terms, in addition to the well-known flux terms. Using the model of Ref. [33] and *in situ* measurements from the THEMIS spacecraft [35], Banerjee *et al.* [36] and Hadid *et al.* [13] evidenced the role of density fluctuations in amplifying the energy cascade rate in the slow wind compared to the fast wind. Hadid *et al.* [37] have further found that density fluctuations reinforce the anisotropy of the energy cascade rate with respect to the local magnetic field in Earth's MS, and evidenced a link with kinetic plasma instabilities. However, those observational works were limited to the inertial range

and used only some of the flux terms (all the source and the majority of the hybrid terms could not have been estimated using single spacecraft data).

In this Letter, we provide the first complete estimation of the compressible turbulent energy cascade rate in the MHD inertial range *and* at the sub-ion scales ($\varepsilon_{\text{CHall}}$) in a collisionless plasma. We use the MMS high time resolution observations made in Earth's MS and an exact relation recently derived for compressible Hall-MHD (HMHD) turbulence [38]. We investigate the impact of the level of density fluctuations on $\varepsilon_{\text{CMHD}}$ and $\varepsilon_{\text{CHall}}$ by their comparison to $\varepsilon_{\text{IMHD}}$ and $\varepsilon_{\text{IHall}}$ obtained, respectively, with incompressible MHD and HMHD theories [15,16,39–41].

Theoretical model.—Using the compressible HMHD equations [42] and following the usual assumptions for fully developed homogeneous turbulence (i.e., infinite kinetic and magnetic Reynolds numbers and a steady state with a balance between forcing and dissipation [32,43]), an exact relation for fully developed turbulence can be obtained [38] as

$$\begin{aligned}
 \varepsilon_{\text{C}} &= \varepsilon_{\text{CMHD}} + \varepsilon_{\text{CHall}} = (\varepsilon_{\text{CMHD}}^{\text{flux}} + \varepsilon_{\text{CMHD}}^{\text{nonflux}}) + (\varepsilon_{\text{CHall}}^{\text{flux}} + \varepsilon_{\text{CHall}}^{\text{nonflux}}) \\
 &= -\frac{1}{4} \nabla_{\ell} \cdot \langle [(\delta(\rho \mathbf{u}) \cdot \delta \mathbf{u} + \delta(\rho \mathbf{u}_A) \cdot \delta \mathbf{u}_A + 2\delta e \delta \rho) \delta \mathbf{u} - [\delta(\rho \mathbf{u}) \cdot \delta \mathbf{u}_A + \delta \mathbf{u} \cdot \delta(\rho \mathbf{u}_A)] \delta \mathbf{u}_A] \\
 &\quad - \frac{1}{4} \left\langle \left(e'_c + \frac{u_A'^2}{2} \right) \nabla \cdot (\rho \mathbf{u}) + \left(e_c + \frac{u_A^2}{2} \right) \nabla' \cdot (\rho' \mathbf{u}') \right\rangle + \frac{1}{4} \langle \beta_i^{-1} \nabla' \cdot (e'_c \rho \mathbf{u}) + \beta_i^{-1} \nabla \cdot (e_c \rho' \mathbf{u}') \rangle \\
 &\quad - \frac{1}{2} \left\langle \left(R'_E - \frac{R'_B + R_B}{2} - E' + \frac{P'_M - P}{2} \right) (\nabla \cdot \mathbf{u}) + \left(R_E - \frac{R_B + R'_B}{2} - E + \frac{P_M - P'}{2} \right) (\nabla' \cdot \mathbf{u}') \right\rangle \\
 &\quad - \frac{1}{2} \langle [R_H - R'_H - \bar{\rho}(\mathbf{u}' \cdot \mathbf{u}_A) + H'] (\nabla \cdot \mathbf{u}_A) + [R'_H - R_H - \bar{\rho}(\mathbf{u} \cdot \mathbf{u}'_A) + H] (\nabla' \cdot \mathbf{u}'_A) \rangle \\
 &\quad - \frac{1}{2} \nabla_{\ell} \cdot \langle [(\overline{\rho \mathbf{J}_c \times \mathbf{u}_A}) \times \delta \mathbf{u}_A - \delta(\mathbf{J}_c \times \mathbf{u}_A) \times \overline{\rho \mathbf{u}_A}] \rangle \\
 &\quad - \frac{1}{2} \left\langle \delta \rho \frac{\mathbf{J}_c \cdot \mathbf{u}'_A}{2} (\nabla \cdot \mathbf{u}_A) - \delta \rho \frac{\mathbf{J}'_c \cdot \mathbf{u}_A}{2} (\nabla' \cdot \mathbf{u}'_A) \right\rangle - \frac{1}{4} \langle (R_B - R'_B) (\nabla \cdot \mathbf{J}_c) + (R'_B - R_B) (\nabla' \cdot \mathbf{J}'_c) \rangle, \quad (1)
 \end{aligned}$$

with, by definition, ρ the mass density, $\mathbf{u}_A \equiv \mathbf{B} / \sqrt{4\pi\rho}$ the compressible Alfvén velocity, $e_c \equiv c_s^2 \log(\rho / \langle \rho \rangle)$ the internal energy, c_s the local sound speed, $\mathbf{J}_c \equiv \mathbf{J} / en$ the compressible electric current, $\mathbf{J} \equiv (c/4\pi) \nabla \times \mathbf{B}$ the current density, n the ion number density, e the electron charge, $P = c_s^2 \rho$ the pressure, $P_M \equiv \rho u_A^2 / 2$ the magnetic pressure, $E \equiv (\rho/2)(\mathbf{u} \cdot \mathbf{u} + \mathbf{u}_A \cdot \mathbf{u}_A) + \rho e$ and $H \equiv \rho(\mathbf{u} \cdot \mathbf{u}_A)$ are, respectively, the one-point total energy and density-weighted cross-helicity per unit volume, $R_E \equiv (\rho/2)(\mathbf{u} \cdot \mathbf{u}' + \mathbf{u}_A \cdot \mathbf{u}'_A) + \rho e'$ and $R_H \equiv (\rho/2)(\mathbf{u} \cdot \mathbf{u}'_A + \mathbf{u}_A \cdot \mathbf{u}')$ are their respective two-point correlation functions, and $R_B \equiv (\rho/2)(\mathbf{u}_A \cdot \mathbf{u}'_A)$ is magnetic energy density. Fields are taken at point \mathbf{x} or $\mathbf{x}' = \mathbf{x} + \ell$; in the latter case a prime is added to the field. The angular brackets $\langle \cdot \rangle$ denote an ensemble average [44], which is taken here as time average assuming ergodicity. We have introduced the usual increments and

local mean definitions, i.e., $\delta\alpha \equiv \alpha' - \alpha$ and $\bar{\alpha} \equiv (\alpha' + \alpha)/2$ (with α any scalar or vector function), respectively.

From Eq. (1), one can notice that the compressible energy cascade rate ε_{C} can be split into two components: a purely MHD component $\varepsilon_{\text{CMHD}}$ (2nd to 5th lines), hereafter, AS17 [34], and a subion one $\varepsilon_{\text{CHall}}$ (6th to 7th lines), hereafter, AGS18 [38], which corresponds to the terms in Eq. (1) proportional to \mathbf{J}_c . In addition, for each component, the cascade can be split into two types of terms: a flux term that can be written as the local divergence of products of two-point increments and nonflux terms that involve spatial divergence of the different fields (e.g., \mathbf{u} , \mathbf{u}_A , or $\rho \mathbf{u}$). The flux terms are the usual terms present in exact laws of incompressible turbulence [15,16]. Assuming isotropy, these flux terms reflect the nonlinear cascade rate of energy through scales, while the nonflux terms act on the inertial

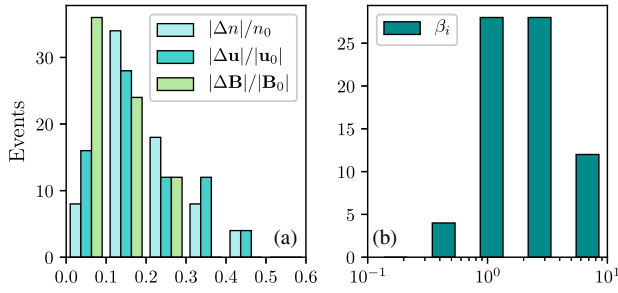


FIG. 1. Histogram for (a) the number density, velocity, and magnetic fluctuations and (b) the ion β_i parameter, respectively.

range as a source or a sink for the mean energy cascade rate, see Refs. [32,34].

Expression (1) is an exact relation describing homogeneous, stationary, isothermal, compressible, HMHD turbulence [38]. It generalizes previous laws [15,16,32–34] by including plasma compressibility, spatial anisotropy, and the Hall effect. On the one hand, when incompressibility is assumed, Eq. (1) reduces to the exact law for incompressible HMHD turbulence with $\varepsilon_I = \varepsilon_{\text{IMHD}} + \varepsilon_{\text{IHall}}$, where $\varepsilon_{\text{IHall}}$ is the contribution of the Hall term, hereafter, F19 [39,41]. On the other hand, for scales larger than d_i (MHD limit), the terms proportional to \mathbf{J}_c go to zero and Eq. (1) converges toward the exact law of CMHD turbulence [33,34].

MMS data selection.—To compute each term in the right-hand side of Eq. (1), we used MMS spacecraft data in burst mode [14] and during intervals of time when it was traveling in Earth’s MS. The magnetic field data and ion plasma moments were measured, respectively, by the Flux Gate Magnetometer (FGM) [45] and the Fast Plasma Investigation (FPI) dual ion/electron sensors (DIS/DES) [46]. The data sampling time is 150 ms, set by the lowest sampling rate, i.e., that of the FPI ion sensor [45].

When we use the Taylor hypothesis on spacecraft measurements, the time sampling of the data is converted into a one-dimensional spatial sampling of the turbulent fluctuations along the flow direction [13,36,47]. Therefore, we had constructed temporal correlation functions of the different turbulent fields at different time lags τ taken within the interval $\sim[0.15\text{--}300]$ s, which allow us to probe into MHD and subion scales. The terms that include divergence of the fields in Eq. (1) (i.e., the source, hybrid, and β -dependent terms), see Refs. [34,38], involve spatial derivatives that were fully computed using the four multispacecraft data of MMS [48]. The electric current comes from the ion and electron moments measured by FPI. The results on the cascade rate were checked against the current estimates given by the curlometer technique [49], and no significant difference was found.

In a large survey of the Cluster data in Earth’s MS, Huang *et al.* [11] found that the magnetic field fluctuations at the MHD scales near the bow shock have generally a power spectral density (PSD) close to f^{-1} , see also

Ref. [50], whose physics is still largely unknown, while those that have a Kolmogorov-like spectrum (i.e., $f^{-5/3}$) were observed toward the flanks of the magnetopause. Since this study focuses on turbulence cascade and uses theoretical models that assume the existence of the inertial range, we selected only cases that showed a Kolmogorov-like spectrum in the MHD scales. However, some spectra showed small bumps near the ion scale, which would reflect the presence of kinetic instabilities [51]. This aspect is not investigated in this first work on subion scale cascade. Our data selection criteria resulted in a total of 72 intervals of ~ 300 s each. In particular, Fig. 1 shows the histograms for (a) the number density, velocity, and magnetic field fluctuations and (b) the ion β_i parameter, respectively.

Results.—For the selected events, we computed the total energy cascade rates ε_C using the exact relation (1) [38]. Figures 2 and 3(c) show two representative examples of both MHD and subion scales’ contributions to the total energy cascade rate from the incompressible and compressible exact relations. We emphasize here that we are only considering the magnitude of the cascade rate rather than its signed value. The latter requires much larger statistical samples to ensure statistical convergence [22,37], which are not yet available to us due to the limited

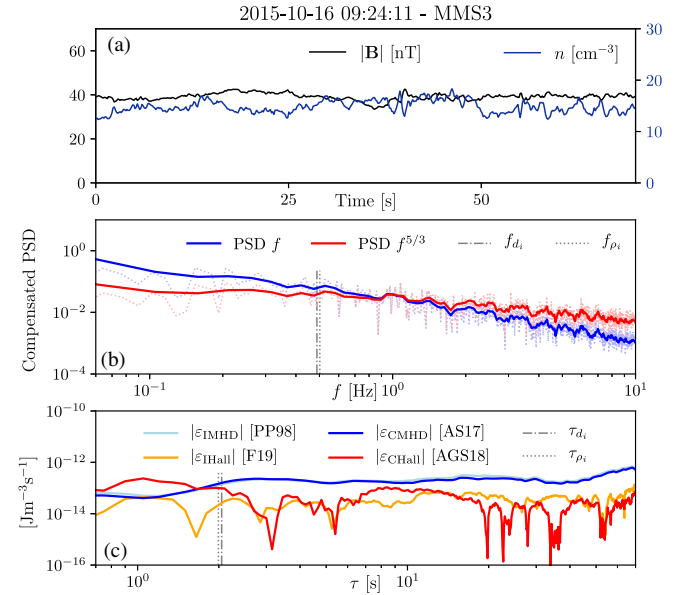


FIG. 2. (a) Magnetic field amplitude (black) and number density (blue), as a function of time. (b) Magnetic field spectra compensated by the power laws f (blue) and $f^{5/3}$ (red), as a function of the frequency f (solid bold line is the average spectrum obtained using a sliding window). (c) Energy cascade rates estimated from incompressible MHD (light blue), incompressible HMHD (orange), compressible MHD (blue), and compressible HMHD (red), as a function of the time lag τ . Vertical dash-dotted and dotted gray lines in (b) and (c) correspond to the Taylor shifted ion skin depth and Larmor radius.

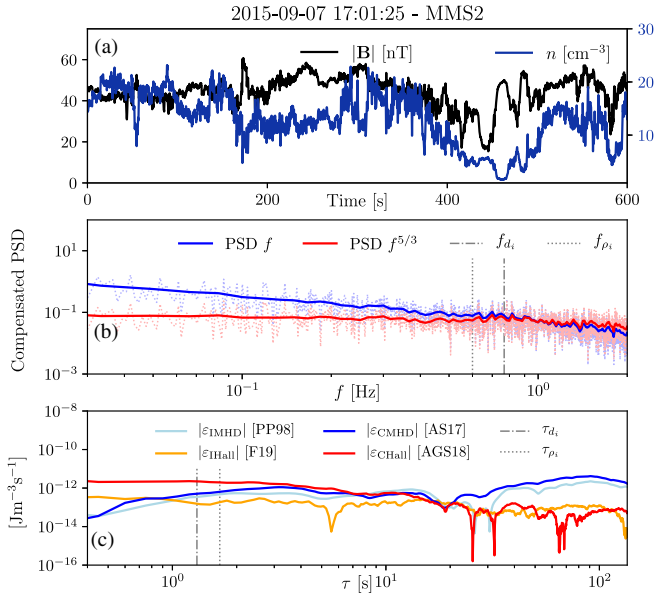


FIG. 3. Same plots as in Fig. 2 but for another time interval.

duration of the burst mode on MMS [14]. Signed cascade rates are relevant to study the direction (i.e., direct vs inverse) of the energy cascade, which is beyond the scope of this Letter.

Figures 2, 3(a), and 3(b) show, respectively, the magnetic field amplitude and number density, and the compensated PSD for the magnetic energy. While both examples show a Kolmogorov-like slope at the largest scales, the level of density fluctuations and its correlation with the magnitude of $|\mathbf{B}|$ are very different. In Fig. 2(a), we observe a relatively uniform $|\mathbf{B}|$, a clear feature of incompressible Alfvénic fluctuations [52], in agreement with the finding of Chen and Boldyrev [53] who analyzed this event: they found the dominance of Alfvénic turbulence at the MHD scales which transitions into KAW near the ion scales. In contrast, Fig. 3(a) shows higher fluctuations in the amplitude of the magnetic field, which are anticorrelated with the density fluctuations. This suggests the dominance of slow-like magnetosonic turbulence [7,51,54].

This is further demonstrated by quantifying separately the contribution of incompressible and compressible fluctuations using the energy cascade rate. In Fig. 2(c), we see that the $|\epsilon_{\text{IMHD}}|$ and $|\epsilon_{\text{CMHD}}|$ almost exactly superimpose to each other at all scales. However, in Fig. 3(c) we observe a larger value of $|\epsilon_{\text{CMHD}}|$ compared to $|\epsilon_{\text{IMHD}}|$. Typically, this increase is due to the compressible flux terms, which include density and internal energy fluctuations [34,55]. While at MHD scales $|\epsilon_{\text{CHall}}|$ and $|\epsilon_{\text{IHall}}|$ in Fig. 2(a) behave similarly, a major difference is observed at subion scales: $|\epsilon_{\text{CHall}}|$ is increasingly larger than $|\epsilon_{\text{IHall}}|$ as one moves towards small scales. This is in agreement with the idea that turbulence transitions into KAW turbulence at these scales [53]. This property is also observed for the case with higher

density fluctuations in Fig. 3 and seems to be a fundamental property of MS turbulence.

This conclusion is clearly demonstrated in Fig. 4, which shows the mean ratios $|\epsilon_{\text{CHall}}|/|\epsilon_{\text{IHall}}|$ as a function of the mean ratios $|\epsilon_{\text{CMHD}}|/|\epsilon_{\text{IMHD}}|$ obtained for all the 72 events that resulted from our data selection. We emphasize that here we considered only cases where the dominant cascade rate components showed an approximately constant (negative or positive) sign for all of the time lags in the MHD and subion ranges to ensure a reliable estimate of its mean values. The mean values at the MHD and sub-ion scales were computed over the time lags $\sim[50-150]$ and $\sim[0.5-5]$ s, respectively. At MHD scales we observe in Fig. 4 that higher density fluctuations lead to increasing $|\epsilon_{\text{CMHD}}|$ over $|\epsilon_{\text{IMHD}}|$. More importantly, we see that even when $|\epsilon_{\text{CMHD}}|/|\epsilon_{\text{IMHD}}| \sim 1$, most of those cases show higher $|\epsilon_{\text{CHall}}|$ compared to $|\epsilon_{\text{IHall}}|$. For some of them, 1 order of magnitude difference between the two cascade rates is seen. These statistical results support the idea that even a small level of density fluctuations could amplify the energy cascade rate as it goes into the subion scales, demonstrating the inherently compressible nature of the MS plasma turbulence at those small scales.

Finally, in Fig. 5 we show the mean ratios in the subion scales $|\epsilon_{\text{CHall}}^{\text{nonflux}}|/|\epsilon_{\text{CHall}}|$ as a function of the mean ratios in the MHD scales $|\epsilon_{\text{CMHD}}^{\text{nonflux}}|/|\epsilon_{\text{CMHD}}|$ obtained for all the 72 events. Similarly to Figs. 2,3(c), we observe that the nonflux terms (i.e., the source, hybrid, and β -dependent [34]) are negligible with respect to the flux

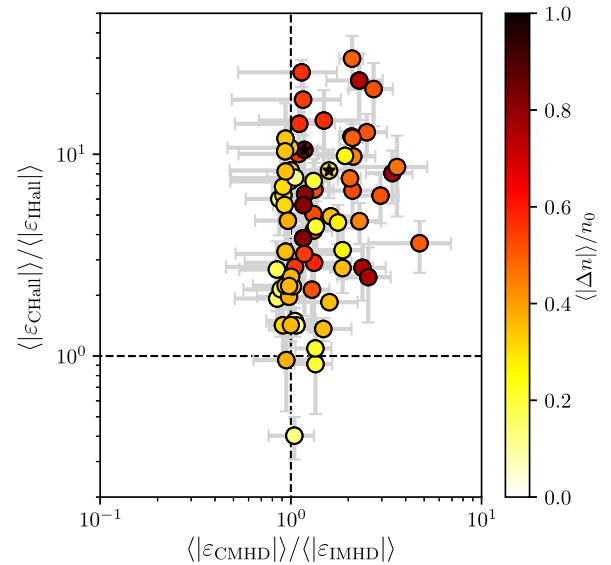


FIG. 4. Mean ratio of the compressible to incompressible cascade rates $|\epsilon_{\text{CHall}}|/|\epsilon_{\text{IHall}}|$ as a function of the mean ratio $|\epsilon_{\text{CMHD}}|/|\epsilon_{\text{IMHD}}|$. The color bar indicates the mean relative density fluctuations per event (72 events are analyzed) in the MS plasma. The error bars are the corresponding standard deviation in the MHD and subion ranges. The stars correspond to cases in Figs. 2 and 3.

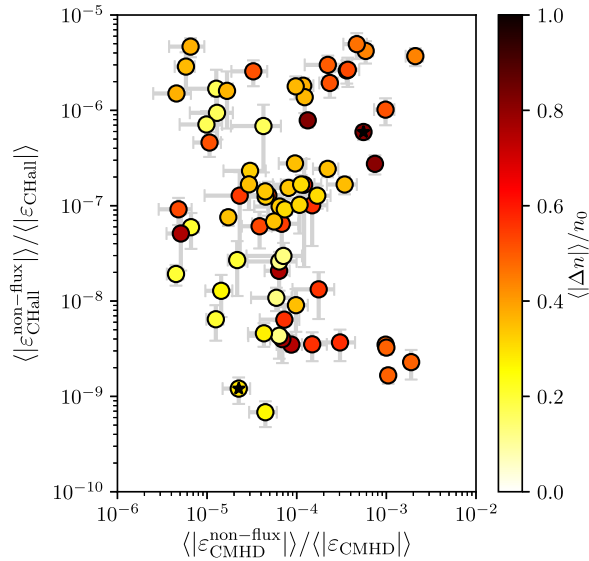


FIG. 5. Mean ratio of the nonflux terms to the compressible cascade rates in the subion scales $\langle |\epsilon_{\text{CHall}}^{\text{non-flux}}| \rangle / \langle |\epsilon_{\text{CHall}}| \rangle$ as a function of ratio in the MHD scales $\langle |\epsilon_{\text{CMHD}}^{\text{non-flux}}| \rangle / \langle |\epsilon_{\text{CMHD}}| \rangle$. The color bar indicates the mean level of density fluctuations per event (72 events are analyzed) in the MS plasma. The error bars are the corresponding standard deviation in the MHD and subion ranges. The stars correspond to cases in Figs. 2 and 3.

terms. These observational results are also corroborated by numerical results previously reported in compressible hydrodynamics and MHD turbulence [55], and in a recent statistical study of the cascade rate at MHD scales using MMS data in the MS [56].

Conclusion.—Understanding sub-ion scale turbulence in space plasmas is a difficult subject because the physics involves many processes that we still do not fully understand. Notably, a fundamental question remains open as to how much energy (stirred up at the large scales) leaks down into the subions, which eventually gets dissipated (by some kinetic processes) into ion and/or electron heating? The subsequent question is how much of that energy comes from the incompressible vs the compressible components of the turbulence? These are fundamental plasma physics questions that are relevant to other distant astrophysical plasmas, e.g., accretion disks of massive objects [57,58]. In this study, we provide some answers to these questions using the MMS data in Earth’s MS and a recent exact law for compressible HMHD, by estimating the first compressible energy cascade rate at subion scales in a collisionless plasma and demonstrating the leading order played by density fluctuations at those scales. The question as to which kinetic processes dissipates energy into particle heating cannot be addressed by our fluid models. Future studies should tackle this problem and the possible role that kinetic instabilities can play in the cascade at subion scales.

Data were obtained from Ref. [59].

N. A. is supported by a DIM-ACAV postdoctoral fellowship. The authors acknowledge the MMS team for producing the data. The authors acknowledge financial support from CNRS/CONICET Laboratoire International Associé (LIA) MAGNETO.

*nandres@iafe.uba.ar, nandres@df.uba.ar

- [1] A. Alexakis and L. Biferale, *Phys. Rep.* **767–769**, 1 (2018).
- [2] S. Galtier, *J. Phys. A* **51**, 293001 (2018).
- [3] A. Pouquet, D. Rosenberg, R. Marino, and C. Herbert, *J. Fluid Mech.* **844**, 519 (2018).
- [4] R. Bruno and V. Carbone, *Living Rev. Solar Phys.* **2**, 4 (2005).
- [5] A. A. Schekochihin, S. C. Cowley, W. Dorland, G. W. Hammett, G. G. Howes, E. Quataert, and T. Tatsuno, *Astrophys. J. Suppl. Ser.* **182**, 310 (2009).
- [6] C. Tao, F. Sahraoui, D. Fontaine, J. de Patoul, T. Chust, S. Kasahara, and A. Retin, *J. Geophys. Res.* **120**, 2477 (2015).
- [7] L. Hadid, F. Sahraoui, K. H. Kiyani, A. Retino, R. Modolo, P. Canu, A. Masters, and M. K. Dougherty, *Astrophys. J. Lett.* **813**, L29 (2015).
- [8] A. Kivelson, *Introduction to Space Physics* (Cambridge University Press, Cambridge, England, 1995).
- [9] P. Song, C. T. Russell, and M. F. Thomsen, *J. Geophys. Res.* **97**, 8295 (1992).
- [10] F. Sahraoui, J. L. Pinon, G. Belmont, L. Rezeau, N. Cornilleau-Wehrin, P. Robert, L. Mellul, J. M. Bosqued, A. Balogh, P. Canu, and G. Chanteur, *J. Geophys. Res.* **108**, 1335 (2003).
- [11] S. Huang, L. Hadid, F. Sahraoui, Z. Yuan, and X. Deng, *Astrophys. J. Lett.* **836**, L10 (2017).
- [12] G. G. Howes, S. D. Bale, K. G. Klein, C. H. K. Chen, C. S. Salem, and J. M. TenBarge, *Astrophys. J.* **753**, L19 (2012).
- [13] L. Hadid, F. Sahraoui, and S. Galtier, *Astrophys. J.* **838**, 9 (2017).
- [14] J. L. Burch, T. E. Moore, R. B. Torbert, and B. L. Giles, *Space Sci. Rev.* **199**, 5 (2016).
- [15] H. Politano and A. Pouquet, *Phys. Rev. E* **57**, R21 (1998).
- [16] H. Politano and A. Pouquet, *Geophys. Res. Lett.* **25**, 273 (1998).
- [17] P. D. Mininni and A. Pouquet, *Phys. Rev. E* **80**, 025401(R) (2009).
- [18] S. Boldyrev, J. Mason, and F. Cattaneo, *Astrophys. J. Lett.* **699**, L39 (2009).
- [19] M. Wan, S. Servidio, S. Oughton, and W. H. Matthaeus, *Phys. Plasmas* **17**, 052307 (2010).
- [20] L. Sorriso-Valvo, R. Marino, V. Carbone, A. Noullez, F. Lepreti, P. Veltri, R. Bruno, B. Bavassano, and E. Pietropaolo, *Phys. Rev. Lett.* **99**, 115001 (2007).
- [21] F. Sahraoui, *Phys. Rev. E* **78**, 026402 (2008).
- [22] J. T. Coburn, M. A. Forman, C. W. Smith, B. J. Vasquez, and J. E. Stawarz, *Phil. Trans. R. Soc. A* **373**, 20140150 (2015).
- [23] J. M. Weygand, W. H. Matthaeus, S. Dasso, M. G. Kivelson, and R. J. Walker, *J. Geophys. Res.* **112**, A10 (2007).
- [24] W. H. Matthaeus, G. P. Zank, C. W. Smith, and S. Oughton, *Phys. Rev. Lett.* **82**, 3444 (1999).
- [25] B. T. MacBride, C. W. Smith, and M. A. Forman, *Astrophys. J.* **679**, 1644 (2008).

- [26] W. H. Matthaeus and M. L. Goldstein, *J. Geophys. Res.* **87**, 6011 (1982).
- [27] F. Sahraoui, S. Galtier, and G. Belmont, *J. Plasma Phys.* **73**, 723 (2007).
- [28] S. Boldyrev and J. C. Perez, *Astrophys. J. Lett.* **758**, L44 (2012).
- [29] J. J. Podesta, *J. Geophys. Res.* **117**, A10106 (2012).
- [30] A. G. Kritsuk, R. Wagner, and M. L. Norman, *J. Fluid Mech.* **729**, R1 (2013).
- [31] V. David and S. Galtier, *Astrophys. J. Lett.* **880**, L10 (2019).
- [32] S. Galtier and S. Banerjee, *Phys. Rev. Lett.* **107**, 134501 (2011).
- [33] S. Banerjee and S. Galtier, *Phys. Rev. E* **87**, 013019 (2013).
- [34] N. Andrés and F. Sahraoui, *Phys. Rev. E* **96**, 053205 (2017).
- [35] H. U. Auster, K. H. Glassmeier, W. Magnes, O. Aydogar, W. Baumjohann, D. Constantinescu, D. Fischer, K. H. Fornacon, E. Georgescu, P. Harvey *et al.*, in *The THEMIS Mission* (Springer, New York, 2009), pp. 235–264.
- [36] S. Banerjee, L. Z. Hadid, F. Sahraoui, and S. Galtier, *Astrophys. J. Lett.* **829**, L27 (2016).
- [37] L. Z. Hadid, F. Sahraoui, S. Galtier, and S. Y. Huang, *Phys. Rev. Lett.* **120**, 055102 (2018).
- [38] N. Andrés, S. Galtier, and F. Sahraoui, *Phys. Rev. E* **97**, 013204 (2018).
- [39] S. Galtier, *Phys. Rev. E* **77**, 015302(R) (2008).
- [40] P. Hellinger, A. Verdini, S. Landi, L. Franci, and L. Matteini, *Astrophys. J. Lett.* **857**, L19 (2018).
- [41] R. Ferrand, S. Galtier, F. Sahraoui, R. Meyrand, N. Andrés, and S. Banerjee, *Astrophys. J.* **881**, 50 (2019).
- [42] S. Galtier, *Introduction to Modern Magnetohydrodynamics* (Cambridge University Press, Cambridge, England, 2016).
- [43] S. Banerjee and A. G. Kritsuk, *Phys. Rev. E* **97**, 023107 (2018).
- [44] G. K. Batchelor, *The Theory of Homogeneous Turbulence* (Cambridge University Press, Cambridge, England, 1953).
- [45] C. T. Russell *et al.*, *Space Sci. Rev.* **199**, 189 (2016).
- [46] C. Pollock *et al.*, *Space Sci. Rev.* **199**, 331 (2016).
- [47] S. Perri, S. Servidio, A. Vaivads, and F. Valentini, *Astrophys. J. Suppl. Ser.* **231**, 4 (2017).
- [48] G. Paschmann and S. Schwartz, in *Cluster-II Workshop Multiscale/Multipoint Plasma Measurements* (ESA Publications Division, 2000), Vol. 449, p. 99.
- [49] M. Dunlop, D. Southwood, K.-H. Glassmeier, and F. Neubauer, *Adv. Space Res.* **8**, 273 (1988).
- [50] W. Macek, A. Krasnińska, M. Silveira, D. Sibeck, A. Wawrzaszek, J. Burch, and C. Russell, *Astrophys. J. Lett.* **864**, L29 (2018).
- [51] F. Sahraoui, G. Belmont, L. Rezeau, N. Cornilleau-Wehrin, J. L. Pinçon, and A. Balogh, *Phys. Rev. Lett.* **96**, 075002 (2006).
- [52] K. H. Kiyani, S. C. Chapman, Y. V. Khotyaintsev, M. W. Dunlop, and F. Sahraoui, *Phys. Rev. Lett.* **103**, 075006 (2009).
- [53] C. H. Chen and S. Boldyrev, *Astrophys. J.* **842**, 122 (2017).
- [54] K. Klein, G. Howes, J. TenBarge, S. Bale, C. Chen, and C. Salem, *Astrophys. J.* **755**, 159 (2012).
- [55] N. Andrés, F. Sahraoui, S. Galtier, L. Z. Hadid, P. Dmitruk, and P. D. Mininni, *J. Plasma Phys.* **84**, 905840404 (2018).
- [56] N. Andrés, F. Sahraoui, S. Galtier, L. Z. Hadid, and R. Ferrand (to be published).
- [57] A. Schekochihin, Y. Kawazura, and M. Barnes, *J. Plasma Phys.* **85**, 905850303 (2019).
- [58] Y. Kawazura, M. Barnes, and A. A. Schekochihin, *Proc. Natl. Acad. Sci. U.S.A.* **116**, 771 (2019).
- [59] See <https://lasp.colorado.edu/mms/sdc/>.